Development of a Self-Balancing Human Transportation Vehicle for the Teaching of Feedback Control

Shui-Chun Lin and Ching-Chih Tsai, *Senior Member, IEEE*

***Abstract*—Control systems education often needs to design interesting hands-on exercises that keep students interested in the control theory presented in lectures. These exercises include system modeling, system analyses, controller syntheses, implementation, experimentation, and performance evaluation of a control system. This paper presents an interesting pedagogical tool, a self-balancing human transportation vehicle (HTV), for the teaching of feedback control concepts in undergraduate electrical, mechatronic, and mechanical engineering environments. Such a pedagogical tool can be easily and inexpensively constructed using low-tech commercial components and feedback control approaches. The effectiveness and performance of the proposed HTV system are examined by conducting several experiments on three different terrains. An education process, together with a pedagogical method, is presented to show how the developed HTV can be incorporated into the laboratory course. To increase students' hands-on experience and keep them interested in learning feedback control, this study also investigated how the enrolled students responded to this new pedagogical tool. This education method along with the HTV system is shown to be significantly effective in helping students to understand feedback control theory and practices, and also to result in more motivated and active learning.**

***Index Terms*—Feedback control, human transportation vehicle, inverted pendulum, phase lead-lag compensation, proportional-derivative control, self-balancing.**

I. Introduction

FEEDBACK control has been extensively taught in many undergraduate engineering curricula, such as electrical engineering, mechanical engineering, mechatronic engineering and so on. Feedback control education often faces the challenging problem of how to give undergraduate students interesting and pragmatic teaching tools by providing hands-on experiments and design problems that complement the theory presented in lectures of control systems or automatic control. In particular, students can greatly benefit if such pedagogical tools are simultaneously applied to dynamic system analysis, control law development, simulation evaluation and experimentation. Furthermore, a significant impression can be made on students if the feedback control concepts presented in class can be easily implemented and the performance of their designed control laws can be evaluated on these teaching tools.

To date, many pedagogical tools have been presented that give undergraduate students hands-on experience on learning the concepts of feedback control [1]–[4]. For instances, they can be inverted pendulums, multi-level water tanks, bicycles, robotic arms, servomotors and so on [4]–[9]. The inverted pendulum control system is one of the most widely used teaching tools all over the world. This type of system, inherently nonlinear and unstable, has been used as a platform or benchmark to investigate the performance of any linear and nonlinear control methods. However, the inverted pendulum system can neither be used to provide more interesting and versatile applications, nor be adopted to examine the performance of any control systems with multiple inputs and outputs. These shortcomings can be avoided if the low-tech bicycle presented in [10] is used, or if the proposed self-balancing human transportation vehicle (HTV) is employed. From the viewpoint of controller design and implementation, the self-balancing HTV is much easier to model and control than the low-tech bicycle. Hence, the goal of this paper is to demonstrate how to develop the proposed self-balancing HTV for teaching feedback control.

Self-balancing HTVs, like the Segway [11], have been well recognized as useful human transportation vehicles. This type of vehicle can be usually constructed by a synthesis of mechatronics, control techniques and software. In contrast to the Segway, several researchers in [12]–[15] have proposed low-tech and low-cost self-balancing HTVs. Blackwell [12] constructed a low-cost self-balancing scooter using the off-the-shelf inexpensive components, but had yet to describe his controller design approach in detail. Grasser *et al.* [13] presented an unmanned mobile inverted pendulum, called JOE; however, JOE was a test prototype, aiming at providing several theoretical design and analytical approaches. Pathak *et al.* [14] and Salerno *et al.* [15], respectively, designed and implemented their self-balancing two-wheeled robots; however, these robots were still scaled-down prototypes. From the view of feedback control education, these inexpensive HTVs, like the pedagogical bicycles in [10] and the well-known inverted pendulums in [4], have high potential to become interesting and practical teaching tools.

The objective of the paper is to study how systematically to construct such a low-cost and pragmatic HTV as a teaching tool,

Manuscript received October 3, 2007; revised March 4, 2008. Current version published February 4, 2009. This work was supported in part by the Ministry of Education, Taiwan, under the ATU plan, and by the National Science Council, Taiwan, by Grant NSC 95-2213-E-005-002.

S. C. Lin was the Department of Electrical Engineering, National Chung Hsing University, Taichung 40227, Taiwan. He is now with the Department of Electrical Engineering, National Chin Yi University of Technology, Taichung 41101, Taiwan.

C.-C. Tsai is with the Department of Electrical Engineering, National Chung Hsing University, Taichung 40227, Taiwan (e-mail: cctsai@dragon.nchu.edu.tw).

Color versions of one or more of the figures in this paper are available online at http://ieeexplore.ieee.org.

Digital Object Identifier 10.1109/TE.2008.921799

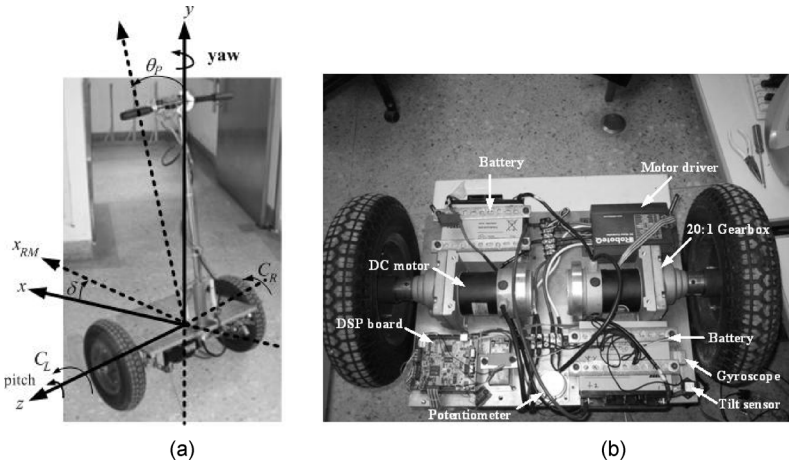

Fig. 1. Experimental self-balancing two-wheeled HTV. (a) Front view. (b) Bottom view.

to investigate how the developed HTV fits in a course structure, and how the enrolled students respond to this new pedagogical tool. Once the system structure and mathematical model of the HTV are described and established, the overall system model will be divided into two subsystems, the yaw control subsystem and the inverted pendulum subsystem, thus leading to the design of two kinds of conventional controllers for yaw control and self-balancing. Through computer simulations and experimentations, the proposed HTV, with the proposed conventional controllers and two gain tuning knobs, will be shown to be useful in achieving satisfactory self-balancing and yaw control performance for different riders. After successful development of the HTV, the teaching of feedback controls using the HTV is investigated by the appropriate educational process, including course description and pedagogical method, and student feedback. The former describes a course whose experimental assignments are covered in a weekly 3-h laboratory, and then explains how the proposed HTV is incorporated into the course and how a pedagogical method is developed to teach the described contents, thereby bringing about an interesting pedagogical environment conducive to learning. The latter presents the course evaluation from the enrolled students at the end of this course, especially for the HTV system. Furthermore, the student feedback also explores how the HTV changes the students' perceptions of feedback control.

Students involved with the use or development procedure of this pedagogical HTV are expected thereby to have strengthened and enhanced their understanding of all the feedback control concepts presented in class, including system structure design, mathematical modeling and conventional controllers design for self-balancing and yaw control, computer simulations, sample-data transformation and experimentations. The design of the proposed HTV can be further used to provide students with vivid and hands-on exercises that prove, or fail to prove, a number of theoretical questions related to the self-balancing HTV's dynamics and control. Questions examined include open-loop stability, step and ramp responses for the HTV, and the effect on dynamic response due to plant variations caused by riders. Furthermore, this proposed teaching tool also helps students to understand two levels of controller synthesis methodology, including: (i) inclusion of simple dynamic compensation, such as PID control and phase lead-lag compensation, and (ii) controller's parameter tuning. This pedagogical experience is thus enhanced because the correlation or lack thereof between the theoretical and the physical is readily accomplished and thus made real to the student. In studying the HTV, the students are systematically exposed to feedback control-related thought processes, becoming comfortable with the abstract methods of feedback control theory as they see complex and opaque topics become clear as a result of application of the feedback control theory. Finally, the proposed teaching tool is designed to act in concert with an appropriate teaching technique, to bring about a pedagogical environment conducive to the learning of feedback control concepts as in Bloom's taxonomy [16], of the six-level hierarchy of knowledge (at the theoretical level), comprehension, application, analysis, synthesis and evaluation.

The rest of this paper is structured as follows. Section II describes the mechatronic design, control architecture and sensing and signal conditioning. Section III is devoted to developing the two conventional controllers for achieving yaw control and self-balancing, and then conducting several simulations to examine the effectiveness of the proposed control methods. Section IV presents several experimental results which are in good agreement with the aforementioned simulation results. The course description and pedagogical method are presented in Section V. Student feedback is given in Section VI. Section VII concludes the paper.

II. System Design

A. Mechatronic Design

Fig. 1 displays the photograph of the proposed HTV with self-balancing two-wheeled mechanism. This type of vehicle is composed of one foot plate, two 24 V_{dc} motors with gearbox and two stamped steel wheels with 16-in tires, two 12 V_{dc} sealed rechargeable lead-acid batteries in series, one motor driver, one digital signal processor (DSP) as a main controller, one handlebar with a potentiometer as a position sensor, one gyroscope and one tilt sensor. The motor driver uses dual H-bridge circuitry to deliver pulsewidth modulation (PWM) power to drive

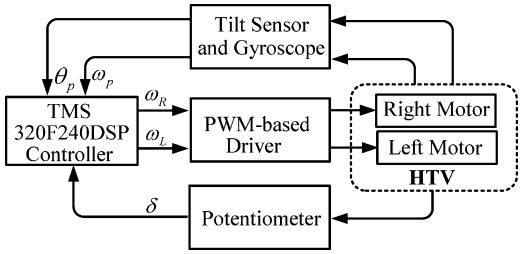

Fig. 2. Block diagram of the entire HTV control system.

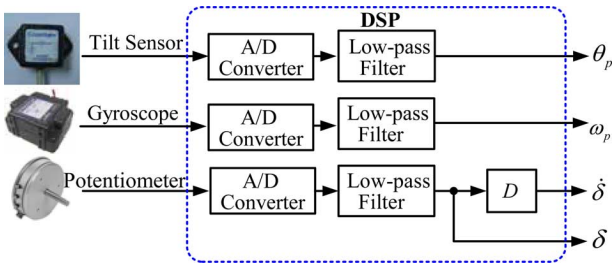

Fig. 3. Block diagram of the sensors and their signal filters.

the two dc motors. Sending PWM signals to the H-bridge circuit, the DSP controls linear speed and yaw rate of the HTV as well as maintains its balance. The gyroscope and the tilt sensor are employed for measuring the rate and the inclination angle of the footplate caused by the rider. The two rechargeable lead-acid batteries directly provide power for the two dc motors and the driver, and for the controller and all the sensors via dc-dc buck converters.

B. Control Architecture

Fig. 2 illustrates the block diagram of the overall HTV control system. The DSP controller, along with built-in A/D converters, is responsible for executing the control algorithms for both self-balancing and yaw control. The feedback signals from the gyroscope and the tilt sensor are used by the controller to maintain the human body on the footplate without falling. The operating principle of the self-balancing control is simply interpreted as below; if the rider leans forward, then the vehicle will move forward in order to maintain the rider without falling, and vice versa. The signal taken from the potentiometer is used in the controller to rotate the yaw axis of the transporter to the desired angle.

C. Sensing and Signal Processing

Fig. 3 shows the block diagram of the sensors and their signal filters. These filters process the measured pitch angle rate ω_P from the gyroscope and the measured pitch angle θ_P from one tilt sensor via the first-order low pass filters, thus removing unwanted signals. The potentiometer is adopted to measure the shaft angle of the handlebar and the angular signal is directly measured by the DSP controller with necessary signal processing.

D. Motors and Their Drivers

The two dc motors used for the HTV are Model NPC T-64 from NPC Company, USA, which have the advantages of simple installation and high torque output and are rated at 24 V_{dc}. These two dc motors were specially chosen not only for their ability to support the load of human riders of various weights, but also for their ability to provide enough power to carry out high-performance driving. For the sake of compactness, such motors are directly coupled to their gearboxes with a gear ratio of 20:1, and then connected to the 16-inch wheels. Note that each motor and its gearbox are put together in one package; this dc motor with gearbox has a maximum speed of 230 RPM, and weights 5.9 kg. The main reason for selecting two16-inch wheels is so that the HTV can safely move over uneven and undulating terrains. It is worth noting that since the electrical time constant of the motor is much faster than the mechanical time constant of the HTV, the modeling process of the HTV will ignore the motor's electrical dynamics.

The commercial motor driver model "AX2550" from Roboteq is used to simultaneously drive both two dc motors by using its PWM input signals. This motor driver can be operated independently, or can be combined to set the forward/reverse direction and steering of the vehicle by coordinating the motor on each side of the vehicle. The motors are driven using high-efficiency Power MOSFET transistors controlled with PWM signals at 10 kHz. The motor power stages can operate from 12 to 40 V_{dc} and can sustain up to 120 A of controlled current.

E. Digital Signal Processor (DSP)

The single-chip DSP TMS320LF2407 from Texas Instruments is used to implement closed-loop control algorithms for the self-balancing HTV. The development environment, called code composer studio, is capable of providing real-time analysis and data verification via JTAG real-time data exchange technology, thus making the debugging process efficient. The fundamental functions to implement the algorithms are listed as follows: (1) analog-to-digital converter (ADC); (2) pulsewidth modulator (PWM). The DSP controller with built-in A/D converter continuously digitizes the time-varying analog signals from the tilt sensor, the gyroscope and the potentiometer. The 10-bit analog-to-digital converter has a minimum conversion time of 375 ns and offers up to 16 channels of analog inputs, in which three channels are adopted to execute the A/D converter from the three sensors mentioned above. The peripherals of the TMS320LF2407 include the event manager module which provides general-purpose timers and compare registers to generate the PWM outputs. Sending appropriate PWM signals to the motor driver, the DSP achieves self-balancing and yaw control of the transporter.

F. Tilt Sensor

The title sensor (CXTA02) from Crossbow Technology is a micro-machined acceleration sensing element with a dc response to measure the footplate's inclination relative to gravity. Mounted beneath the footplate [see Fig. 1(b)], the sensor measures the pitch angle of the footplate and outputs an offset voltage plus the voltage response proportional to the sine of the inclination angle of the HTV.

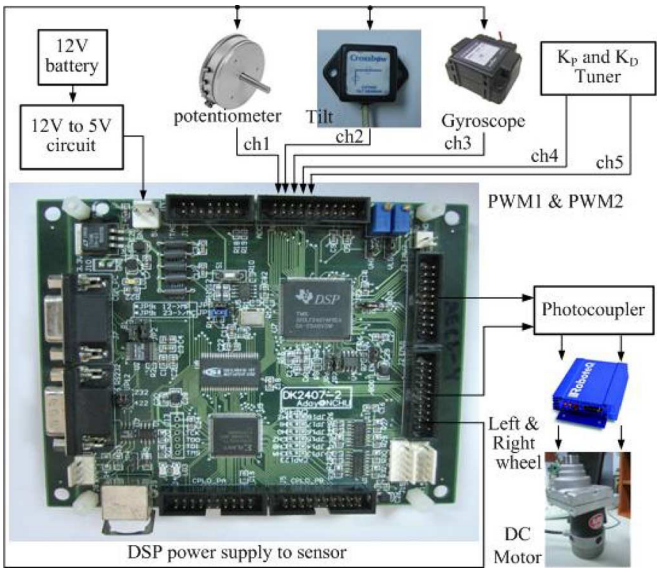

Fig. 4. Overall system structure and its wire connections.

G. Potentiometer

This potentiometer is used as a steer-bar position sensor for yaw-axis rotation, and functions as a variable resistance structure. When a 5 V_{dc} voltage source is added between its terminals, the potentiometer outputs a variable voltage corresponding to the actual position associated with the steer-bar.

H. Rate Gyroscope

The piezoelectric vibration rate gyroscope used is the model ENV-05H-02 Gyrostar from Murata Electronics. The rate gyroscope is mounted beneath the footplate [see Fig. 1(b)] and adopted to measure the HTV's pitch rate ranging from -90 deg/sec to 90 deg/sec, and then gives the output signal ranging from 0.502 to 4.498 V_{dc} in which 2.5 V_{dc} means that the footplate is at zero angular velocity.

I. Power Supply System

The main power supply consists of two 12 V, 22 Ah batteries in series, which can deliver sufficient power to drive the two motors. The power supply for the DSP comes from an extra power source with isolated ground. The DSP controller only outputs the control signal from 0 to 3.3 V_{dc} and the motor driver only accepts the input signal from 0 to 5 V_{dc},, thus requiring a voltage conversion circuitry. This voltage conversion can be easily accomplished by using a TTL input CMOS buffer such as, for example, 74HCT244.

J. Overall System Architecture

Fig. 4 displays the overall system architecture for the HTV. In this diagram, the outputs of the potentiometer, the tilt sensor and the gyro are respectively connected to channels ch1, ch2, and ch3 of the ADC. In addition, two knobs are adopted to tune the two controller parameters, such as the proportional and derivative gains, and the phase lead-lag controller's gain. The outputs of the knobs are connected to channels ch4 and ch5 in the ADC.

III. Controllers Design and Simulation Results

A. Two Decoupled Subsystems

This section will briefly describe the two decoupled subsystems of the HTV with coulomb friction between the wheels and the surface. Appendix A1 details how to establish the simplified mathematical model of the HTV without external disturbance forces and the dynamics of the motors. With the well-known decoupling matrix technique, the overall system of the HTV system can be decomposed into two independent subsystems: the mobile inverted pendulum subsystem described by

$$\begin{pmatrix} \dot{\theta}_P \\ \dot{\omega}_P \end{pmatrix} = \begin{pmatrix} 0 & 1 \\ A_{43} & 0 \end{pmatrix} \begin{pmatrix} \theta_P \\ \omega_P \end{pmatrix} + \begin{pmatrix} 0 \\ B_4 \end{pmatrix} C_\theta \tag{1}$$

and the yaw control subsystem governed by

$$\begin{pmatrix} \dot{\delta} \\ \ddot{\delta} \end{pmatrix} = \begin{pmatrix} 0 & 1 \\ 0 & A_{66} \end{pmatrix} \begin{pmatrix} \delta \\ \dot{\delta} \end{pmatrix} + \begin{pmatrix} 0 \\ B_6 \end{pmatrix} C_\delta. \tag{2}$$

The controlled torque C_θ is synthesized to maintain the mobile inverted pendulum subsystem without falling at any small inclination angles imposed by the rider, and the controlled torque C_δ is designed to achieve the yaw control. Note that both controllers can be designed separately and then combined to carry out any desired motion imposed by the rider.

For the mobile inverted pendulum subsystem, the control goal of the subsystem is to achieve self-balancing without falling down, i.e., to stabilize itself at the origin. For the developed yaw control subsystem with the potentiometer as the main sensor, the yaw rate control problem can be reduced to a regulation problem, because the potentiometer merely measures the yaw rate error between the yaw rate the rider intended to achieve, and the measured yaw rate of the mobile platform. For this kind of yaw control, the angular command or reference is always set to be zero. This simple yaw control system thus avoids the use of another gyroscope for measuring the yaw angle of the HTV.

B. Conventional Controller Design

Proportional-integral-derivative (PID) control and phase lead-lag compensation have been not only widely used in industrial control systems for achieving setpoint (or trajectory) tracking and regulation, but also extensively taught in feedback control courses [1], [2], due to their simple structure, robustness against plant variations, and easy parameter tuning. PID control generates control signals that are proportional to the error between the reference signal and the actual output (proportional action), to the integral of the error (integral action), and to the derivative of the error (derivative action), thereby providing the desired control performance if the three-term parameters (proportional, integral and derivative gains) are well designed or tuned. Many classical and advanced methods [17]–[19] have been proposed to design or tune these parameters in order to achieve the desired transient and steady-state performance specifications. Similar to PID control, phase lead-lag compensators have also three-term tuning parameters: control gain, and zero and pole locations. Also having the advantage of high frequency noise attenuation, they have also been used to meet required performance specifications for tracking and regulation. In this section, proportional derivative (PD) and phase lead-lag

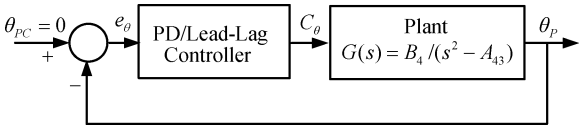

Fig. 5. Block diagram of the PD/phase lead-lag self-balancing control subsystem.

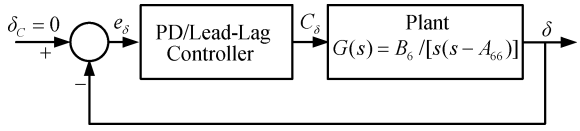

Fig. 6. Block diagram of the PD/phase lead-lag yaw control subsystem.

controllers will be analytically synthesized to steer the proposed HTV, by selecting the appropriate controller parameters such that the closed-loop systems have the required characteristic equations, satisfying the given transient specifications.

1) Self-Balancing Controller Design: This subsection will consider the design of these two conventional controllers for the self-balancing of the inverted pendulum subsystem in torque level. The conventional PD controller is presented first and the conventional phase lead-lag controller is then proposed, with both design procedures being described using the transfer function approach.

PD Self-Balancing Controller Design: The PD self-balancing controller is intended to maintain the mobile inverted pendulum subsystem at $\theta_{PC} = 0$ with zero steady-state error and to provide the desired transient performance. Fig. 5 depicts the block diagram of the PD self-balancing controller where the PD controller is represented by $G_c(s) = K_{P\theta} + K_{D\theta}s$, and the inverted pendulum subsystem is described by $G(s) = B_4/(s^2 - A_{43})$, where the two parameters B_4 and A_{43} are found in Appendix A1. The aim of the PD controller design is to determine the control parameters $K_{P\theta}$ and $K_{D\theta}$ such that the closed-loop system is asymptotically stable, and the closed-loop characteristic equation equals the desired second-order characteristic equation.

From Fig. 5 the Mason gain formula is used to obtain the closed-loop transfer function as follows:

$$G_{overall}(s) = \frac{(K_{P\theta} + K_{D\theta}s)\,B_4}{s^2 + K_{D\theta}B_4 s + (B_4K_{P\theta} - A_{43})}. \quad (3)$$

To stabilize the closed-loop system and obtain the desired transient performance simultaneously, let the closed-loop characteristic equation equal the desired second-order characteristic equation, namely that

$$s^2 + K_{D\theta}B_4 s + (B_4K_{P\theta} - A_{43}) = s^2 + 2\xi\omega_n s + {\omega_n}^2 \quad (4)$$

where ω_n and ζ are the desired natural frequency and damping ratio. By comparing the coefficients of the second-order polynomials in two sides, one obtains

$$K_{P\theta} = \frac{({\omega_n}^2 + A_{43})}{B_4} \quad \text{and} \quad K_{D\theta} = \frac{2\xi\omega_n}{B_4}. \quad (5)$$

Since the pitch command is set by zero, i.e., $\theta_{PC} = 0$, then $e_\theta = -\theta_P$.The transfer function of the PD controller, described by $C_\theta(s) = (K_{P\theta}+K_{D\theta}s)e_\theta(s)$ can be obtained via the inverse Laplace transform.

$$C_\theta(t) = -(K_{P\theta}\theta_P(t) + K_{D\theta}\omega_P(t)). \quad (6)$$

Phase Lead-Lag Self-Balancing Controller Design: The subsection aims to synthesize a phase lead-lag self-balancing controller so as to regulate the mobile inverted pendulum to $\theta_{PC} = 0$ with the same performance mentioned before. As shown in Fig. 5, where the phase lead-lag self-balancing controller is used, it is possible to obtain the following closed-loop transfer function via block diagram reduction method or the Mason gain formula:

$$G_{overall}(s) = \frac{k_\theta(s + z_\theta)B_4}{s^3 + p_\theta s^2 + (k_\theta B_4 - A_{43})s + (k_\theta B_4 z_\theta - p_\theta A_{43})}. \quad (7)$$

To stabilize the closed-loop inverted pendulum subsystem and attain the desired transient performance simultaneously, the closed-loop characteristic equation can be made to equal the desired third-order characteristic equation satisfying the integral of time multiplied by the absolute error (ITAE) criterion [17]–[19], i.e., $s^3 + 1.75\omega_n s^2 + 2.15{\omega_n}^2 s + {\omega_n}^3 = 0$.

Hence

$$s^3 + p_\theta s^2 + (k_\theta B_4 - A_{43})s + (k_\theta B_4 z_\theta - p_\theta A_{43}) = s^3 + 1.75\omega_n s^2 + 2.15{\omega_n}^2 s + {\omega_n}^3 \quad (8)$$

which yields

$$k_\theta = \frac{(2.15{\omega_n}^2 + A_{43})}{B_4}, \quad p_\theta = 1.75\omega_n,$$
$$z_\theta = \frac{({\omega_n}^3 + 1.75\omega_n A_{43})}{(2.15{\omega_n}^2 + A_{43})}. \quad (9)$$

2) Yaw Controller Design: The objective of the subsection is to develop simple PD and phase lead-lag control rules for the yaw control subsystem. As mentioned before, the yaw control problem is reduced to a regulation problem. Thus, this subsection will repeat the design procedures of the self-balancing controller design above by finding appropriate two-term parameters for the PD and phase lead-lag controller. Unlike the inverted pendulum subsystem which is of type 0, the yaw control subsystem is of type 1, such that the controller's parameters are different from those for the inverted pendulum subsystem.

PD Yaw Controller Design: Fig. 6 shows the block diagram of the PD yaw controller where the PD controller is expressed by $G_C(s) = K_{P\delta} + K_{D\delta}s$, and the rotation subsystem is governed by $G(s) = B_6/(s(s - A_{66}))$ where the two parameters B_6 and A_{66} are already given in Appendix A1. By the previous PD self-balancing design procedure the appropriate control parameters $K_{P\delta}$ and $K_{D\delta}$ are easily found such that the closed-loop system is asymptotically stable and the closed-loop characteristic equation equals the desired second-order characteristic equation. From Fig. 6, the closed-loop transfer function for yaw control can be obtained

$$G_{\text{overall}}(s) = \frac{(K_{P\delta} + K_{D\delta}s)\,B_6}{s^2 + (K_{D\delta}B_6 - A_{66})\,s + K_{P\delta}B_6} \quad (10)$$

which gives

$$K_{P\delta} = \frac{{\omega_n}^2}{B_6} \quad \text{and} \quad K_{D\delta} = \frac{(A_{66} + 2\xi\omega_n)}{B_6}. \tag{11}$$

Due to the fact that the rotation command is $\delta_c = 0$, then $e_\delta = -\delta$ where δ is the output of the potentiometer. The time-domain expression of the PD controller is described by

$$C_\delta(t) = -\left(K_{P\delta}\delta(t) + K_{D\delta}\dot{\delta}(t)\right). \tag{12}$$

Phase Lead-Lag Yaw Controller Design: This subsection will establish the phase lead-lag control rule for the yaw control subsystem, easily done by following the phase lead-lag self-balancing controller design. Fig. 6 illustrates the block diagram of the phase lead-lag yaw controller. The controller design procedure is given briefly below. It follows from Fig. 6 that the closed-loop transfer function of the proposed phase lead-lag controller is given by the subsequent third-order system

$$G_{overall}(s) = \frac{K_\delta\,(s + p_\delta)\,B_6}{s^3 + (z_\delta - A_{66})\,s^2 + (K_\delta B_6 - A_{66} z_\delta)\,s + p_\delta K_\delta B_6}. \tag{13}$$

To make the system asymptotically stable and regulate the system in a desired manner, one obtains

$$s^3 + (z_\delta - A_{66})\,s^2 + (K_\delta B_6 - A_{66} z_\delta)\,s + p_\delta K_\delta B_6 = s^3 + 1.75\omega_n s^2 + 2.15{\omega_n}^2 s + {\omega_n}^3. \tag{14}$$

Solving (14) yields

$$z_\delta = 1.75\omega_n + A_{66},\ K_\delta = \frac{\left(2.15{\omega_n}^2 + A_{66}(1.75\omega_n + A_{66})\right)}{B_6},$$
$$p_\delta = \frac{{\omega_n}^3}{\left(2.15{\omega_n}^2 + A_{66}(1.75\omega_n + A_{66})\right)}. \tag{15}$$

Results and Discussion of Simulation: This section examines the effectiveness and performance of the proposed two control methods for the self-balancing HTV by conducting computer simulations on a personal computer using the MATLAB package. Using the parameters given in Table I and (A.2) in the Appendix to this paper gives the values $A_{43} = 140$, $A_{66} = -0.8$, $B_4 = -0.0204$ and $B_6 = -0.0204$,, which are employed in these simulations. These simulations considered the performance of the proposed conventional controllers for a rider with a known weight and the rider's tilt and yaw control commands applied to the HTV. Fig. 7(a) illustrates the simulation block diagrams of the PD self-balancing regulator and the PD yaw control regulator under three cases: underdamped, critically damped, and overdamped. Figs. 8(a) and 9(a) respectively depict the simulation results of the proposed PD self-balancing and yaw controllers when a forward-backward move command and then a left-right yaw command were applied to the HTV. The result in Fig. 8(b) indicates that the proposed conventional PD self-balancing controller with the appropriate parameters is capable of providing satisfactory regulation performance but with a steady-state error, whereas the result in Fig. 9(b) reveals that the proposed conventional PD yaw controller has satisfactory regulation performance without any steady-state error. Similarly, Fig. 7(b) presents the block diagrams for simulating the phase lead-lag controllers for self-balancing and yaw control for three different natural frequencies. Figs. 10(a) and 11(a), respectively, illustrate the simulation results of the two phase lead-lag compensators; the results in Figs. 10(b) and 11(b) show that both compensators have steady-state errors, and the errors decreases as the natural frequency increases.

TABLE I
SYMBOLS DEFINITION

Symbol and unit	Measured Value	Parameter and variable name
x_{RM} [m], v_{RM} [m/s]	–	movement position and speed of the Chassis
θ_p[rad], ω_p [rad/s]	–	pitch angle, pitch angular velocity
δ [rad], $\dot{\delta}$ [rad/s]	–	yaw angle, yaw angular velocity
C_L[N·m]	–	applied torque on left wheel
C_R [N·m]	–	applied torque on right wheel
J_{RR} [kg·m^2], J_{RL} [kg·m^2]	0.11	Moment of inertia of the rotation mass with respect to the z axis
M_{RR} [kg], M_{RL} [kg]	5.5	Mass of the rotation mass connected to the left and right wheel
$J_{p\theta}$ [kg·m^2]	27.6	Moment of inertia of the chassis with respect to the z axis
$J_{p\delta}$ [kg·m^2]	3.478	Moment of inertia of the chassis with respect to the y axis
M_p [kg]	135	Mass of the chassis with the weight of the rider (80kg)
R [m]	0.2	Radius of the wheels
D [m]	0.6	Lateral distance between the contact patches of the wheels
L [m]	1	Distance between the z axis and the CG of the chassis
b	0.01	Friction coefficient
n	20	Gear ratio

IV. EXPERIMENTAL RESULTS AND DISCUSSION

The objective of the experiments is to examine the performance of the proposed PD and phase lead-lag control laws for achieving self-balancing and yaw control. The performance of these controllers for the HTV is evaluated on three different terrains: smooth, uneven and ramp terrains. The performance of such controllers for different riders and different terrains can be adjusted by tuning the two knobs so as to alter directly the controllers' parameters, the proportional and derivative gains, and the phase lead-lag controller's gain. In addition, since all the control and signal filtering rules are executed by the DSP-based controller, they must be transformed into their digital forms. Appendix A2 details the digitization procedure to obtain the corresponding difference equations of these controllers designed in Section III.

A. Experimental Results of the Proposed Self-Balancing Controllers

The real-time control codes of the proposed PD and phase lead-lag self-balancing controllers were implemented by stan-

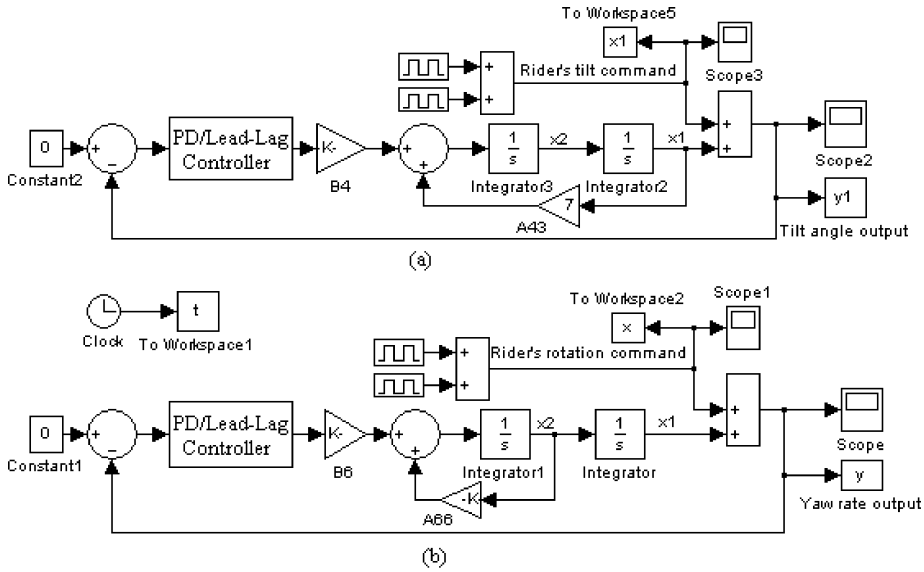

Fig. 7. Simulation Block diagrams. (a) PD/phase lead-lag self-balancing controller. (b) PD/phase lead-lag yaw regulators.

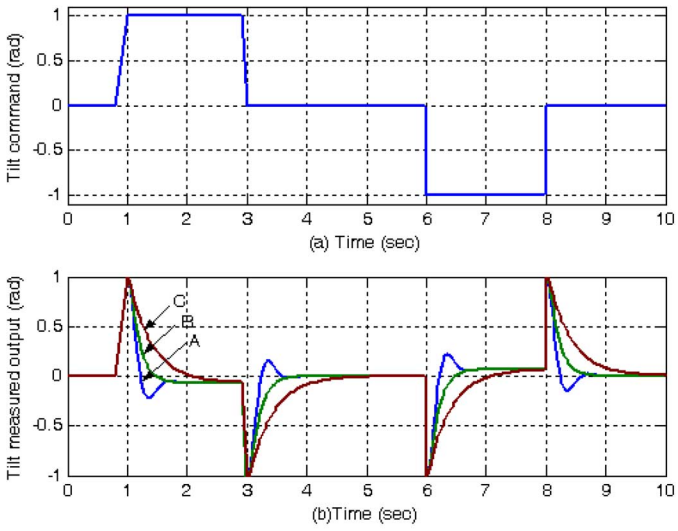

Fig. 8. Transient performance of the PD self-balancing regulator. (a) Tilt commands. (b) Simulated tilt output for three cases. Case A: $\zeta = 0.5$ (underdamped) and $\omega_n = 10\ \mathrm{rad/sec}$; Case B: $\zeta = 1$ (critically damped) and $\omega_n = 10\,\mathrm{rad/sec}$; Case C: $\zeta = 2$ (overdamped) and $\omega_n = 10\,\mathrm{rad/sec}$.

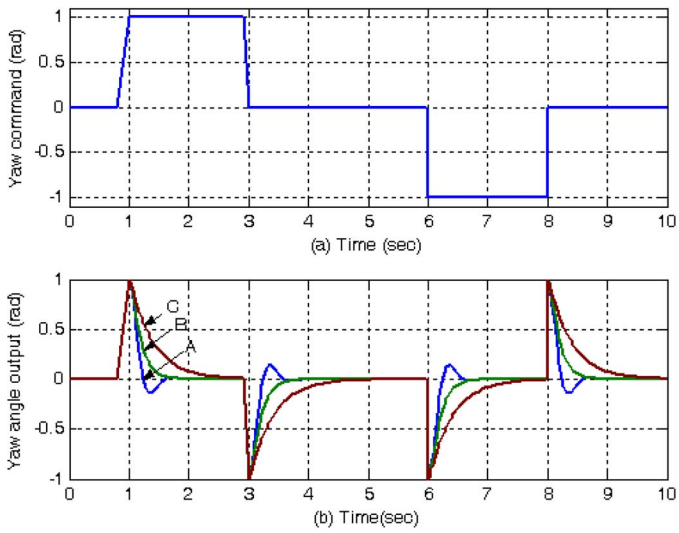

Fig. 9. Transient performance for the PD yaw regulator. (a) Yaw commands. (b) Simulated yaw output for three cases. Case A: $\zeta = 0.5$ (underdamped) and $\omega_n = 10\,\mathrm{rad/s}$; Case B: $\zeta = 1$ (critically damped) and $\omega_n = 10\,\mathrm{rad/s}$; Case C: $\zeta = 2$ (overdamped) and $\omega_n = 10\ \mathrm{rad/s}$.

dard C language. Fig. 12 shows the HTV ridden by students while the vehicle was moving forwards and backwards on the smooth floor. From actual riding experience, it seems that the PD controller outperforms the phase lead-lag controller in a large inclination error, and the phase lead-lag controller is superior to the PD controller in a small inclination error.

From these self-balancing control experiments, it appeared that the PD controller has a faster response than the phase lead-lag controller. This result is due to the fact that the PD controller has the advantage of increasing system bandwidth, thus improving the system response. However, for the case when the control rod is either pulled back or pushed forward near the origin, the HTV will exhibit a shaking phenomenon. This shaking phenomenon may be attributed to the derivative effect on self-balancing, and can be interpreted as below. Assume that the HTV is operated near the origin condition, and the tilt error $e_\theta(t)$ is very small, but the derivative of the tilt error $e_\theta(t)$ can be large, and can be positive or negative, depending the operation condition. This large derivative requires a significant control effort to achieve self-balancing in the neighborhood of the origin.

Although the phase lead-lag balancing controller can prevent high-frequency noise from causing shaking near the origin, it has the disadvantage of giving a slow response for the HTV while it is moving forwards or backwards in a larger inclination error. This dilemma is addressed by combining the two controllers for operation in different ranges of the inclination error. For example, the phase lead-lag controller can be used in a small inclination error near the origin, and the PD controller can be adopted to cope a large tilt error. Since the linear angular range

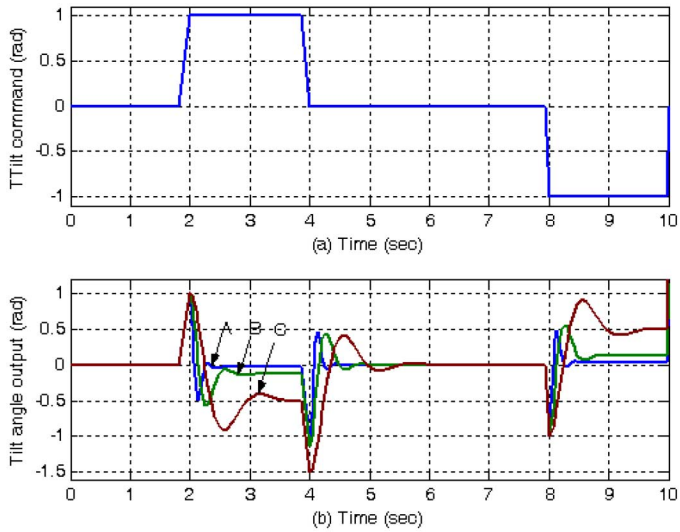

Fig. 10. Transient performance for the phase lead-lag self-balancing regulator. (a) Tilt commands. (b) Simulated tilt output for three cases. Case A: $\zeta = 1$ and $\omega_n = 20$ rad/s; Case B: $\zeta = 1$ and $\omega_n = 10$ rad/s; Case C: $\zeta = 1$ and $\omega_n = 5$ rad/s.

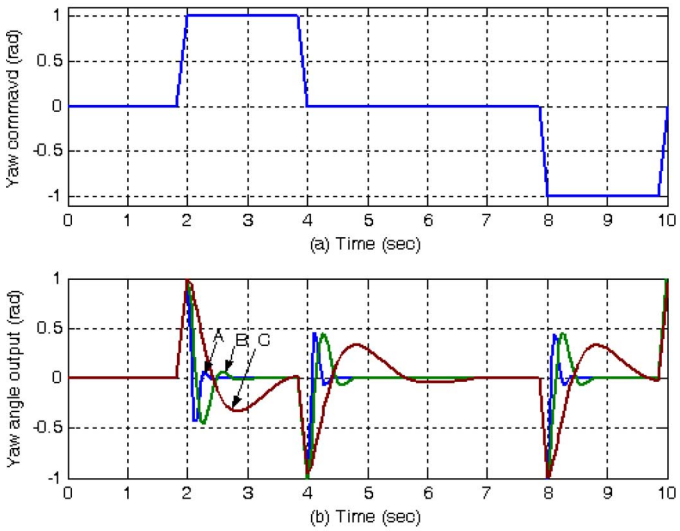

Fig. 11. Transient performance for the phase lead-lag yaw regulator. (a) Yaw commands. (b) Simulated yaw output for three cases. Case A: $\zeta = 1$ and $\omega_n = 20$ rad/s; Case B: $\zeta = 1$ and $\omega_n = 10$ rad/s; Case C: $\zeta = 1$ and $\omega_n = 5$ rad/s.

of the tilt sensor is from -20 degrees to $+20$ degrees, the suggestion is to use the phase lead-lag controller in a narrow region from -5 degrees to 5 degrees, and to employ the PD controller in other intervals outside this narrow region.

B. Experimental Results of the Proposed Yaw Controllers

Two experiments were conducted to verify the performance of the designed PD and phase lead-lag yaw controllers. In order to perform the experiments, the sampled data transformations of the two controllers were obtained using the backward difference and bilinear transform methods, and the digital control laws were coded by standard C language. Fig. 13 shows the HTV ridden by students while it was turning right and left.

Fig. 12. The HTV ridden by students on a smooth floor. (a) Moving forward. (b) Moving backward.

Fig. 13. The HTV ridden by students while rotating on the smooth floor. (a) Turning left. (b) Turning right.

Fig. 14. The HTV moving on uneven and ramp terrains. (a) Going uphill. (b) Going downhill.

C. Experimental Results of the HTV on Three Different Terrains

The performance of the HTV was investigated with a human rider on three different terrains: smooth floor, uneven road and ramp terrain. Three experiments were conducted with the combined PD and phase lead-lag self-balancing controller and the PD yaw controller. The HTV was safely steered on the smooth floor and a student comfortably rode the HTV on the uneven and ramp terrains, as shown in Fig. 14.

The human riding experience suggested that riding on the smooth floor be much easier than on the uneven or ramp terrain. It is worthwhile mentioning that when the HTV went uphill on the uneven or ramp terrain, the rider required a large tilt angle, but needed a small tilt angle for going downhill. This result is

attributed to the fact that the centre of gravity of the HTV is vertical to the flat ground, but not to the ramp terrain.

V. Course Description and Pedagogical Method

In the one-semester course Automatic Engineering Practices (EE-3362), as taught at the National Chung Hsing University, Taiwan, the enrolled students are required to attend a weekly 3-h laboratory. Those students are advised to take 3-hour lecture each week on feedback control theory before attending the laboratory. The laboratory is taught by teaching assistants under supervision of a control-orientated professor. The activities in the laboratory are classified into three parts; Part I is concerned with computer aided system simulations using the MATLAB package, and Part II puts emphasis on designs of conventional controllers (PID controllers, phase lead-lag compensators, state-feedback controllers) based on the root-locus approach, the frequency-response method, the state-space technique and the MATLAB package. After finishing Part II, in Part III the students are grouped and guided in applying these techniques to analyze various interesting control plants which can be provided in the laboratory, to design PID controllers, phase lead-lag compensators and state feedback controllers, to evaluate the transient and steady-state performance of the designed controllers using MATLAB, and finally to conduct appropriate experiments to examine the performance of their synthesized controllers. In Part III, students in each group are required to give oral presentations of their final course projects using the MS PowerPoint package, and oral defenses of their reports if questions are asked by other students. In order to facilitate the education process, the students are provided prepared handouts for each of the approximately 11 laboratory exercises in Parts I and II, and the five laboratory exercises in Part III.

The proposed HTV has been evaluated by students as one of the most interesting control test platforms, which include inverted pendulums, bicycles, robotic arms, dc servomotors, and so on. The teaching materials for the HTV system are extensively used throughout the laboratory exercises. The HTV's two subsystems are also considered in Parts I and II as illustrative examples to teach digital system simulation, analytical methods, conventional controllers design and performance evaluation. At the start of Part III, the students, choosing the HTV as their final course project are required to research and write an essay dealing, typically, with some open-ended HTV-related topics, such as "explain how a HTV works", "what are the main differences between a bicycle and a HTV?", "why is a HTV much easier to control than a bicycle in [10]?", "what potential applications could there be for the HTV?". After this exercise, these students are quickly exposed to interactions between theoretical thinking and practical issues. Theoretical topics covered in lectures, but which have a bearing on the HTV, include mathematical modeling, the Laplace transform, transient responses, stability tests, root locus, conventional control laws, state feedback, and frequency-domain considerations. These theoretical topics follow in a logical manner, and the student comes to view these topics as part of feedback control theory. Once the notation of the HTV system has been established in the students' minds, additional theoretical tools such as root locus, frequency response, and conventional control laws will be readily accepted. Afterwards, the aforementioned simulation and conventional controller design methods are employed by students to accomplish the PD controller and the phase lead-lag compensator for self-balancing and yaw control, and then examine their performance using MATLAB. The actual performance of the designed controllers is exemplified by conducting several experiments on the experimental HTV, as shown in Section IV.

The authors have made an effort to have a supply of HTVs on hand because they can be easily constructed using the off-the-shelf components. However, the cost of these raw materials for constructing HTVs is not cheap in comparison with the bicycle used as a pedagogical tool in [10]. For the sake of experimental economics, the mechanical fabrication and installation of the proposed HTVs are performed in the machine shop at the National Chung Hsing University, Taiwan, and the students are encouraged to perform digital simulation and develop control laws using MATLAB, code them by using standard C programming techniques, and then do associated experiments. Notice that, in order to avoid unnecessary equipment damage caused by students' carelessness, all the experiments are conducted only after the experimental setup and control codes have been approved by the teaching assistants. At the end of the course the students have designed all the control-oriented pieces in the HTV project and have completed and verified the system.

TABLE II
Student Feedback

Questions	5	4	3	2	1
The contents of the handouts for the HTV are well-developed.	69%	15%	12%	4%	0%
The level of the handouts for the HTV is adequate.	78%	13%	6%	3%	0%
Relevance of the HTV system in the laboratory	62%	21%	16%	1%	0%
The teaching of the feedback control using the HTV is clearly presented.	73%	17%	6%	4%	0%
I gained usefully practical skills from the HTV.	77%	13%	8%	2%	0%
I gained usefully theoretical skills from the conventional controller design for the HTV.	67%	13%	14%	6%	0%
Experience gained with MATLAB/Simulink in class work for the HTV.	76%	18%	5%	1%	0%
Benefits from the final course project in using the HTV to lean feedback control theory and practices.	81%	7%	9%	3%	0%
Overall evaluation.	72%	18%	7%	3%	0%

VI. Student Feedback

This section briefly presents and discusses the course evaluation from the enrolled students at the end of this course, especially for the use of the proposed HTV system. The course evaluation was based on a set of questionnaire shown in Table II with an average of 21 students enrolled each semester. Overall,

the student responses to the proposed laboratory activities were quite positive. From this evaluation, it was concluded that after completion of the laboratory experiments using the HTV system, most of the students considered it to be an effective teaching tool to help them to understand the basic ideas behind feedback control theory and practices. With the HTV system, the students had a stronger motivation to learn digital system simulations, design conventional controllers and then evaluate their performance and effectiveness, conduct the relevant experiments and interpret and analyze experimental data, and gain usefully theoretical and practical skills.

VII. Conclusion

This paper has described the development of a pedagogical self-balancing two-wheeled human transportation vehicle for the teaching of feedback control. The mechatronic method was used to construct the vehicle using off-the-shelf inexpensive components, including the self-balancing two-wheeled motion mechanism, the control architecture using digital signal processing, the power circuitry, and the sensor system used for measuring all the feedback signals, such as the pitch angle and its rate, the yaw angle and rate. With the division of the overall system into two subsystems: the yaw control subsystem and the mobile inverted pendulum subsystem, the PD and phase lead-lag controllers were successfully designed to maintain the HTV without falling and to achieve the desired yaw rate tracking. Through simulations and experimental results, the proposed controllers have been shown to be useful and effective in providing appropriate control actions to steer the vehicle at slow speeds with the desired performance. Moreover, the proposed HTV has also been successfully tested by students on three different terrains.

For educational purposes, the proposed HTV was introduced into an undergraduate laboratory course in feedback control. The proposed education method and process using the HTV received significantly positive responses from the students, thus indicating the strengths of the proposed teaching tool used in the course. The use of the proposed HTV as a concrete and interesting example of a feedback control system not only permits undergraduate students effectively to improve their theoretical understanding and mastery of feedback control technology, but also helps them to have hands-on experience of working on a complete analysis and design procedure of a feedback control system. Hence, most of the students can improve their professional confidence as a result of this substantive and meaningful educational experience.

Appendix

Simplified Mathematical Modeling: Appendix A1 will describe the simplified mathematical model of the HTV with the Coulomb friction between the wheels and the surface. Here, the friction under consideration is assumed to depend on the speed of the transportation vehicle and to be opposite to the direction of motion, i.e., the fiction force on each wheel is proportional to the wheel speed, and the transporter does not slip. In order to simplify the derivation of the modeling processing, Table I lists all the symbols and their definitions and Fig. 1 depicts the definitions of the state variables. The mathematical model of the HTV without external disturbance forces is modified from Grasser *et al.* [13] using the Newtonian mechanism, and its linearized model about $x_{RM}=0$, $v_{RM}=0$, $\theta_p=0$ and $\delta=0$ is then governed by the following state equation:

$$\dot{\mathbf{X}}=\begin{bmatrix}0&1&0&0&0&0\\0&A_{22}&A_{23}&0&0&0\\0&0&0&1&0&0\\0&0&A_{43}&0&0&0\\0&0&0&0&0&1\\0&0&0&0&0&A_{66}\end{bmatrix}\mathbf{X}+\begin{bmatrix}0&0\\B_{21}&B_{22}\\0&0\\B_{41}&B_{42}\\0&0\\B_{61}&B_{62}\end{bmatrix}\begin{bmatrix}C_L\\C_R\end{bmatrix} \tag{A.1}$$

where $\mathbf{X}=[x_{RM}\quad v_{RM}\quad \theta_p\quad \omega_p\quad \delta\quad \dot{\delta}]^T$ denotes the state vector; the parameters in (A.1) are given as

$$\begin{aligned}&A_{22}=\frac{-nR^2}{J_R}\frac{b}{\alpha},\ A_{23}=-\frac{nR^2}{2J_R}\frac{\gamma}{\alpha\beta},\ A_{43}=\frac{n\gamma}{J_{P\theta}}\left(1-\frac{L}{\beta}\right)\\&A_{66}=-n\left(\frac{D^2b+2b_\delta}{2J_{P\delta}p}\right),\ B_{21}=B_{22}=\frac{nR}{2J_R}\left[\frac{1}{\alpha}+\frac{R}{\alpha\beta}\right]\\&B_{41}=B_{42}=\frac{n}{J_{P\theta}}\left(\frac{L}{\beta}-1\right),\ B_{61}=-B_{62}=\frac{nD}{2pJ_{P\delta}R}\end{aligned} \tag{A.2}$$

where $p=1+D^2\cdot\left(J_R+M_RR^2\right)/2J_{p\delta}R^2$, $\alpha=M_RR^2/J_R+1$, $\beta=J_{P\theta}/M_PL+L$, $\gamma=LM_Pg$. Using the facts that $B_2=B_{21}=B_{22}$, $B_4=B_{41}=B_{42}$, $B_2=B_{21}=B_{22}$, $B_4=B_{41}=B_{42}$, $B_6=B_{62}=-B_{61}$, and the well-known decoupling matrix developed in [13]

$$\begin{pmatrix}C_L\\C_R\end{pmatrix}=\begin{pmatrix}0.5&0.5\\0.5&-0.5\end{pmatrix}\begin{pmatrix}C_\theta\\C_\delta\end{pmatrix} \tag{A.3}$$

one decomposes system (A.1) into two independent subsystems: one is concerned with the mobile inverted pendulum subsystem describing the rotation about the z axis, i.e.

$$\begin{pmatrix}\dot{x}_{RM}\\\dot{v}_{RM}\\\dot{\theta}_P\\\dot{\omega}_P\end{pmatrix}=\begin{pmatrix}0&1&0&0\\0&A_{22}&A_{23}&0\\0&0&0&1\\0&0&A_{43}&0\end{pmatrix}\begin{pmatrix}x_{RM}\\v_{RM}\\\theta_P\\\omega_P\end{pmatrix}+\begin{pmatrix}0\\B_2\\0\\B_4\end{pmatrix}C_\theta \tag{A.4}$$

and the other is the yaw control subsystem about the y axis, i.e.

$$\begin{pmatrix}\dot{\delta}\\\ddot{\delta}\end{pmatrix}=\begin{pmatrix}0&1\\0&A_{66}\end{pmatrix}\begin{pmatrix}\delta\\\dot{\delta}\end{pmatrix}+\begin{pmatrix}0\\B_6\end{pmatrix}C_\delta \tag{A.5}$$

where $A_{43}>0$, $B_4<0$, $A_{66}<0$, and $B_6>0$. From (A.3) and (A.5), it is clear that two controllers for C_θ and C_δ can be designed independently from each other and combined together to accomplish the control goal.

Worth mentioning is that the controlled torque C_θ is applied to maintain the mobile inverted pendulum subsystem at the inclination angle imposed by the rider; hence the torque C_θ is designed via the following simplified equation:

$$\begin{pmatrix}\dot{\theta}_P\\\dot{\omega}_P\end{pmatrix}=\begin{pmatrix}0&1\\A_{43}&0\end{pmatrix}\begin{pmatrix}\theta_P\\\omega_P\end{pmatrix}+\begin{pmatrix}0\\B_4\end{pmatrix}C_\theta. \tag{A.6}$$

Note that $A_{43}>0$ and $B_4<0$. Moreover, from (A.4), one finds that once the pitch angle ω_p and the linear speed of the vehicle v_{RM} have reached steady-state values, i.e., $\dot{\omega}_p=0$ and $\dot{v}_{\mathrm{RM}}=0$, then $C_\theta=-A_{43}\theta_p/B_4$ and the vehicle will stabilize the vehicle at a steady-state constant speed $v_{\mathrm{RMss}}=(A_{43}B_2-B_4A_{23})\theta_p/A_{22}B_4$. This result means that when the

rider maintains his pitch angle at a specified angle θ_p, the vehicle must run at a constant speed v_{RMss} in order to stabilize the system without falling.

Digitization of the PD and Phase Lead-Lag Controllers: As mentioned in the body of this paper, all the control and signal filtering rules are executed by the DSP-based controller. Therefore, all the developed controllers must be transformed into their digital versions. There are many existing numerical approximation methods for sampled-data transformation, such as standard z-transform, backward difference, forward difference, Simpson's rule, bilinear z-transform, matched z-transform, and etc, [20]. In particular, backward difference and bilinear z-transform are regarded as two of the most practical numerical approximations in all aspects of digital control applications, and used to digitize the two proposed analog controllers.

Digitization of the PD Controllers By Backward Difference Method: Using the backward difference method and selecting the sampling period as T ($T = 10\,\mathrm{ms}$), one obtains the discrete-time version of the analog PD self-balancing control law (6) as follows:

$$C_\theta(k) = -(K_{P\theta}\theta_P(k) + K_{D\theta}\omega_P(k)) \tag{A.7}$$

where $C_\theta(k)$ and $\theta_P(k)$ respectively represent the sampled data of $C_\theta(t)$ and $\theta_P(t)$ at the kth sampling instant, $t = kT$, $k \in I$. Similarly, the PD yaw controller (12) is digitized by

$$C_\delta(k) = -\left[K_{P\delta}\delta(k) + K_{D\delta}(\delta(k) - \frac{\delta(k-1))}{T}\right]. \tag{A.8}$$

Digitization of the Phase Lead-Lag Controllers By Bilinear Transformation: The basic technique for digitizing the two phase lead-lag control laws for self-balancing and yaw control is to substitute $s = \left[2(1-z^{-1})\right] \cdot \left[T(1+z^{-1})\right]^{-1}$ into the proposed phase lead-lag controllers, thus finding their discrete- time domain expressions. The bilinear transform method is applied to accomplish the task for the phase lead-lag self-balancing controller first and then for the phase lead-lag yaw controller.

For digitization of the phase lead-lag self-balancing controller using the bilinear transform method, the following discrete-time difference equation is obtained at the torque level. As shown in (A.9) at the bottom of the page, where the three parameters k_θ, z_θ, and p_θ are given in (9), and $e_\theta(k) = -\theta_P(k)$. Repeating the same procedure digitizes the phase lead-lag yaw control law and yields the following result, [see (A.10) at the bottom of the page], where the three parameters k_δ, z_δ, and p_δ are given in (15), and $e_\delta(k) = -\delta(k)$.

Digitization of the Torque-to-Speed Conversion: Owing to the fact the DSP-based controller is designed for carrying out the speed tracking control of the dc motors, rather than for direct torque control, the torque obtained in the previous section can not be straightforwardly applied. In addition, a torque-to-speed conversion is required to calculate the speed commands for the motors. From (A.10), one finds the torque for the left wheel

$$C_L(k) = \frac{(C_\delta(k) + C_\theta(k))}{2} \tag{A.11}$$

and the torque for the right wheel

$$C_R(k) = \frac{(C_\theta(k) - C_\delta(k))}{2}. \tag{A.12}$$

Note that, for the sake of low cost and easy implementation, the digital controller does not directly use the torque controller's structure with current feedback; the DSP-based controller employs PWM driving technology to fulfil the speed tracking. The speed commands can be achieved from Newton's second law for yaw control, thus, giving

$$C_L = J_L \cdot \alpha = J_L \cdot \dot{\omega}_L \tag{A.13}$$

which leads to the following digital velocity commands for the left motor using the backward difference

$$\omega_L(k) = \omega_L(k-1) + \frac{(T \cdot C_L(k))}{J_L}. \tag{A.14}$$

Proceeding with the same procedure for digital velocity commands for the right motor yields

$$\omega_R(k) = \omega_R(k-1) + \frac{(T \cdot C_R(k))}{J_R}. \tag{A.15}$$

The results in (A.14) and (A.15) reveal that once both the torques for the right and left wheels have been obtained from (A.11) and (A.12), the digital velocity commands for both motors will be immediately computed via (A.14) and (A.15). The commands are then input to the two independent, digital open-loop speed loops, thereby accomplishing the self-balancing and yaw control actions.

Real-Time Control Algorithm: For implementation of the proposed PD and phase lead-lag control algorithms, the following steps are presented in order to minimize the computation delay problem.

Step1 *: Read the signals form the tilt sensor and the potentiometer via the AD conversion of the DSP-based controller.*

$$C_\theta(k) = \frac{\left\{k_\theta\left[\left(\left(\frac{2}{\mathrm{T}}\right) + z_\theta\right)e_\theta(k) + \left(z_\theta - \left(\frac{2}{\mathrm{T}}\right)\right)e_\theta(k-1)\right] - \left(p_\theta - \left(\frac{2}{\mathrm{T}}\right)\right)C_\theta(k-1)\right\}}{\left[\left(\frac{2}{\mathrm{T}}\right) + p_\theta\right]} \tag{A.9}$$

$$C_\delta(k) = \frac{\left\{k_\delta\left[\left(\left(\frac{2}{\mathrm{T}}\right) + z_\delta\right)e_\delta(k) + \left(z_\delta - \left(\frac{2}{\mathrm{T}}\right)\right)e_\delta(k-1)\right] - \left(p_\delta - \left(\frac{2}{\mathrm{T}}\right)\right)C_\delta(k-1)\right\}}{\left[\left(\frac{2}{\mathrm{T}}\right) + p_\delta\right]} \tag{A.10}$$

Step2 *: Compute* $C_\theta(k)$ *and* $C_\delta(k)$ *of the PD controller from (A.7) and (A.8), or* $C_\theta(k)$ *and* $C_\delta(k)$*of the phase lead-lag compensator from (A.9) and (A.10).*

Step3 *: Calculate the motor's speed commands from (A.11) and (A.12), (A.14) and (A.15)*

Step4 *: Output the motor's speed PWM commands.*

Step5 *: Wait for next sampling instant, and go to Step 1.*

Notice that the aforementioned real-time algorithm is designed based on the principle that the control action must be finished within the first 10% of each sampling interval, and the remaining time is employed to calculate other functions.

REFERENCES

[1] R. Kelly and J. Moreno, "Learning PID structures in an introductory course of automatic control," *IEEE Trans. Educ.*, vol. 44, pp. 373–376, Nov. 2001.

[2] J. C. Basilio and S. R. Matos, "Design of PI and PID controllers with transient performance specification," *IEEE Trans. Educ.*, vol. 45, pp. 364–370, Nov. 2002.

[3] J. R. Rowland, "Integrating lifelong learning into a feedback controls course," in *Proc. Frontiers in Educ. Conf., FIE '99. 29th Ann.*, Nov. 1999, vol. 2, pp. 12b6/13–19.

[4] M. E. Magana and F. Holzapfel, "Fuzzy-logic control of an inverted pendulum with vision feedback," *IEEE Trans. Educ.*, vol. 41, pp. 165–170, May 1998.

[5] M. Mazc, M. Mazo, J. Urena, F. J. Rodriguez, J. J. Garcia, J. L. Lazaro, E. Santiso, F. Espinosa, R. Garcia, P. Revenga, J. C. Garcia, E. Bueno, and R. Mateos, "Teaching equipment for training in the control of DC, brushless, and stepper servomotors," *IEEE Trans. Educ.*, vol. 41, pp. 146–158, May 1998.

[6] M. H. Knudsen, "Experimental modeling of dynamic systems: An educational approach," *IEEE Trans. Educ.*, vol. 49, pp. 29–38, Feb. 2006.

[7] V. A. Oliveira, E. S. Tognetti, and D. Siqueira, "Robust controllers enhanced with design and implementation processes," *IEEE Trans. Educ.*, vol. 49, pp. 370–382, Aug. 2006.

[8] D. J. Lim, "A laboratory course in real-time software for the control of dynamic systems," *IEEE Trans. Educ.*, vol. 49, pp. 346–354, Aug. 2006.

[9] W. K. Chen and Y. C. Cheng, "Teaching object-oriented programming laboratory with computer game programming," *IEEE Trans. Educ.*, vol. 50, pp. 197–203, Aug. 2007.

[10] R. E. Klein, "Using bicycles to teach system dynamics," *IEEE Contr. Syst. Mag.*, vol. 19, no. 3, pp. 4–9, 1989.

[11] Segway Simply moving Segway Inc., 2007 [Online]. Available: http://www.segway.com

[12] T. Blackwell, Building a Balancing Scooter, 2007 [Online]. Available: http://www.tlb.org/scooter.htm

[13] F. Grasser, A. D. Arrigo, and S. Colombi, "JOE: A mobile, inverted pendulum," *IEEE Trans. Ind. Electron.*, vol. 49, pp. 107–114, Feb. 2002.

[14] K. Pathak, J. Franch, and S. K. Agrawal, "Velocity and position control of a wheeled inverted pendulum by partial feedback linearization," *IEEE Trans. Robot. Autom.*, vol. 21, pp. 505–513, Jun. 2005.

[15] A. Salerno and J. Angeles, "The control of semi-autonomous self-balancing robots undergoing large payload-variations," in *Proc. 2004 IEEE Int. Conf. Robot. Autom.*, Apr.-May 6, 2004, vol. 2, pp. 740–1745.

[16] *Taxonomy of Education Objectives*, B. Bloom, Ed. New York: Longmans, Green, 1956.

[17] R. C. Dorf and R. H. Bishop, *Modern Control Systems*, 10th ed. Englewood Cliffs, NJ: Prentice-Hall, 2005.

[18] B. C. Kuo and F. Golnaraghi, *Automatic Control Systems*, 8th ed. New York: Wiley, 2003.

[19] G. F. Franklin, J. D. Powell, and A. Emami-Naeini, *Feedback Control of Dynamic Systems*, 4th ed. Englewood Cliffs, NJ: Prentice-Hall, 2002.

[20] C. L. Phillips and H. T. Nagle, *Digital Control System Analysis and Design*, 3rd ed. Englewood Cliffs, NJ: Prentice-Hall, 1995.

Shui-Chun Lin received the B.S. degree in electronic engineering from National Taiwan University of Science and Technology, Taipei, Taiwan, in 1988, the M.S. degree in electrical engineering from National Chung-Hsing University, Taichung, Taiwan, in 2002.

He is currently working toward the Ph.D. degree with the Department of Electrical Engineering, National Chung-Hsing University. Since 1991, he has been a senior lecturer with the Department of Electronic Engineering, National Chin-Yi University of Technology, Taichung. His current research interests include nonlinear Control, adaptive control, sliding mode control, and their applications to mechatronics and mobile robots.

Ching-Chih Tsai (S'90–M'91–SM'00) received the Diplomat degree in electrical engineering from the National Taipei Institute of Technology, Taipei, Taiwan, the M.S. degree in control engineering from National Chiao-Tung University, Hsinchu, Taiwan, and the Ph.D. degree in electrical engineering from Northwestern University, Evanston, IL, in 1981, 1986, and 1991, respectively.

Currently, he is a Professor with the Department of Electrical Engineering, National Chung-Hsing University, Taichung, Taiwan.

Dr. Tsai served as Chair of the Taipei chapter, IEEE Control Systems Society, from 2001 to 2003, and, from 2003 to 2005, he served as the Director of the Centre for Research Development and Engineering Technology, College of Engineering, National Chung-Hsing University. In 2006, he served as Chair of the Taipei chapter, IEEE Robotics and Automation Society, and Director of the Centre for Advanced Industry Technology and Precision, National Chung-Hsing University. Since 2007, he has been Chair of the Taichung chapter, the Chinese Institute of Engineers.